Holographic spectral beamsplitting for increased organic photovoltaic conversion efficiency

Shelby D. Vorndran*[a], Silvana Ayala[b], Yuechen Wu[b], Juan M. Russo[b], Raymond K. Kostuk[a,b], Jacob T. Friedlein[c], Sean E. Shaheen[c], Christine K. Luscombe[d]

[a]College of Optical Sciences, The University of Arizona, Tucson, Arizona 85721, USA; [b]Department of Electrical and Computer Engineering, The University of Arizona, Tucson, Arizona 85721, USA; [c]Department of Electrical, Computer, and Energy Engineering, University of Colorado at Boulder, Boulder, Colorado 80309, USA; [d]Materials Science and Engineering Department, University of Washington, Seattle, Washington 98195-2120, USA

ABSTRACT

Thermodynamic principles limit the conversion efficiency of a single bandgap organic photovoltaic (OPV) cell to 33%[1]. In order to increase efficiency, multiple OPV devices can be combined to cover a larger spectral range of the incident solar spectrum. The most common way of doing this is to mount multiple bandgap cells in tandem or series. However, stacked multijunction systems have limitations, such as current-matching constraints and optical quality of the OPV layer. A separated arrangement with spectrum splitting is a promising alternative to the stacked tandem approach. In this paper, two organic photovoltaic cells with complementary EQE curves are integrated into a holographic spectrum splitting module. The highest possible conversion efficiency of this two-cell combination is quantified assuming an ideal spectral filter as a reference. A spectrum splitting module is built, consisting of a reflective hologram oriented at an angle to split the incident beam into two spectral bands. The holographic beamsplitting system is assembled and studied under a solar simulator. Power output and conversion efficiency of the holographic spectrum splitting system is evaluated in terms of Improvement over Best Bandgap (IoBB) of the two-cell combination. The combined system has a measured improvement over its best single cell of 12.30% under a solar simulator lamp and a predicted improvement of 16.39% under sunlight.

Keywords: Solar energy, organic photovoltaic, holographic optical element, spectrum splitting, light management

1. INTRODUCTION

In an effort to reduce the cost of renewable energy, inexpensive photovoltaic materials have been developed. Organic photovoltaic (OPV) cells have a low material cost and a streamlined manufacturing process. However, the conversion efficiency of these devices is still quite low, with highest efficiencies of 10-12% and typical values of 5-8% efficiency[2]. Power conversion efficiency is limited by several factors, one of the most significant being the narrow absorption spectra of organic materials[3]. By combining multiple OPV devices with absorption covering the entire solar spectrum, efficiency can be increased dramatically. One approach to multiple-bandgap OPV is a stacked multijunction arrangement. This type of cell has been fabricated and tested over the years with mixed results. While some stacked multijunction cells show improvement[4], others perform at the same efficiency or even a lower efficiency than a single cell under the full spectrum[3]. Optimizing the OPV layers and intermediate electrode layers for current matching in the stack is one of the greatest difficulties. In addition, non-optimal optical transparency can further reduce output of the bottom cell[3].

*Further author information:
S. D. V.: E-mail: shelbyv@email.arizona.com, Telephone: 1 260 414 9022

Organic Photovoltaics XV, edited by Zakya H. Kafafi, Paul A. Lane, Ifor D. W. Samuel, Proc. of SPIE Vol. 9184, 918423 · © 2014 SPIE
CCC code: 0277-786X/14/$18 · doi: 10.1117/12.2061773

To address these challenges, a spectrum splitting approach can be taken. Spectrum splitting utilizes an optical element to spatially redistribute the solar spectrum onto appropriate PV cells. By separating the solar cells, the issue of optical transparency and current matching is avoided. Previous work by the authors involved characterizing a reflective holographic spectrum splitting system for Gallium Arsenide and Silicon photovoltaic cells[5]. In the current work, this holographic system will be applied to two OPV cells (P3HT:ICBA and PSiFBT:PCBM). Conversion efficiency of the combined system will be compared to that of the most efficient OPV cell operating under the full spectrum.

2. OPV AND REFLECTION HOLOGRAM COMPONENTS

2.1 OPV Cell Fabrication and Characterization

The active-layer materials used in the OPV devices are poly(3-hexylthiophene) (P3HT), PSiFBT, a copolymer of a silicon-containing multifused thienyl-fluorene-thienyl and benzothiadiazole synthesized through Stille coupling[6], indene-C_{60} bisadduct (ICBA), and [6,6]-phenyl-C_{61}-butyric acid methyl ester (PCBM). OPV devices were fabricated using an inverted geometry of ITO/ZnO/active-layer/MoOx/Ag. The ZnO layer was formed from a zinc acetate precursor solution spin-coated and thermally converted in air to produce a film with thickness of ~40 nm. The active layer of P3HT:ICBA, 1:1 by weight with a total concentration 34 mg/mL, was spin-coated from dichlorobenzene at 800 rpm, and slow-dried to a thickness of ~200 nm. The active layer of PSiFBT:PCBM, 3:10.5 by weight with a total concentration 13.5 mg/mL, was spin-coated from chlorobenzene at 800 rpm to a thickness of ~100 nm. MoOx was thermally deposited under high-vacuum at a rate of 0.1 Å/s to a total thickness of either 20 nm (for P3HT:ICBA devices) and 10 nm (for PSiFBT:PCBM devices). Ag was thermally deposited at a rate of 1 Å/s to a thickness of 100 nm for all devices. All fabrication steps after ZnO conversion were performed in nitrogen glove boxes. The final devices were encapsulated with a cover slip and UV epoxy for subsequent characterization and spectrum splitting implementation in ambient atmosphere.

Electrical properties of the P3HT:ICBA and PSiFBT:PCBM cells were measured (Table 1). The spectral responsivity of the cells was characterized using a monochromator (Figure 1). Maximum efficiency gain in a spectrum splitting system occurs when PV cells have no overlap in their spectral responsivity. While these cells show some, there is still a spectral range over which the multijunction system can provide measurable improvement.

Table 1. Electrical properties of OPV cells used. The cells have an active area of 0.11 cm^2.

OPV Cell	I_{SC} (mA)	V_{OC} (V)	P_{MP} (mW)	Fill Factor	η
P3HT:ICBA	0.8129	0.56	0.2701	0.5933	2.46%
PSiFBT:PCBM	0.6876	0.84	0.2867	0.4964	2.61%

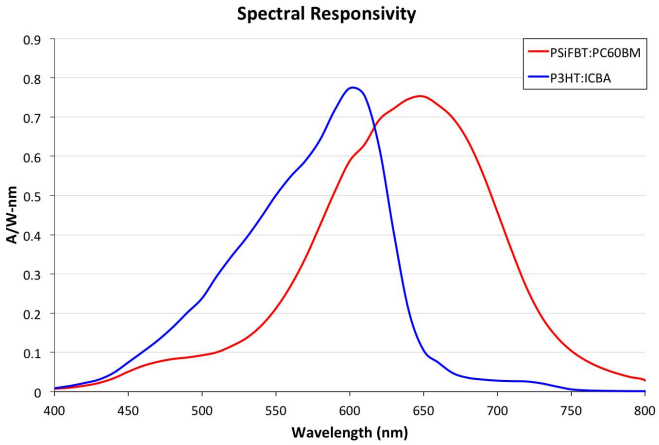

Figure 1. Measured spectral responsivity of OPV solar cells used in spectrum splitting application.

2.2 Reflection Hologram Fabrication and Characterization

Volume reflection holograms reflect a chosen wavelength range and transmit all other wavelengths. This spectral filter can be used as a beam-splitting element if oriented at an angle. The holograms fabricated in our lab are made from dichromated gelatin (DCG), a material that can achieve high reflectance (up to 100%) with little scattering and absorption loss. DCG also has good environmental stability if sealed properly[7].

A DCG film consisting of 12% gelatin and 2% ammonium dichromate by weight to water was mold-coated onto a glass substrate. After 1 day of drying and hardening, the film was exposed using a 532 nm laser with output irradiance of 5 mW/cm^2. The DCG plate was indexed matched onto the diagonal face of a prism, allowing recording angles of +/- 49° in glass. The recording angle was chosen to properly relate recording wavelength and film swelling percentage to the desired reflected wavelength and angle. The interference pattern between incident and reflected light was recorded as a sinusoidal modulation along the normal direction of the film plane. An exposure time of 150 s yielded the best result. The film was developed in a wet process. First, the plate is fixed and hardened for 1.5 minutes in Kodak fixer A and B at 25° C. Next, it is swelled for 1 minute in a water rinse at 25° C, and dehydrated for 30 s in three isopropanol alcohol baths of increasing temperature and concentration (50% at 25° C, 75% at 35° C and 99% at 45° C). Finally, the DCG plates were baked at a temperature of 65° C for 15 minutes to remove any residual water.

The hologram was characterized by measuring spectral transmittance at various angles using a spectrometer. Because the volume hologram acts as a thin-film stack, there is polarization dependence to reflectance. DCG holograms have reduced reflectance for TM light that varies based on incident angle. TM reflectance nearly disappears at 39° incidence. At 45° incidence, the TM reflectance contribution has a narrow bandwidth and reduced peak value. Because of this characteristic, the beamsplitting hologram will be designed to reflect at an angle of incidence somewhat larger than 45° for a more broad and rectangular reflectance curve (Figure 2). The final transmittance curve is shown in Figure 3.

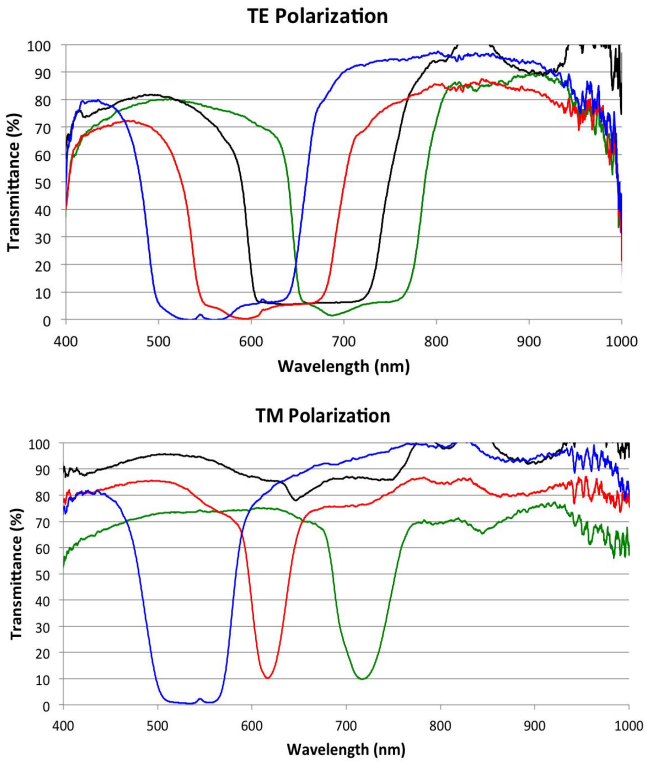

Figure 2. Spectral transmittance graphs for TE and TM polarizations taken for various angles, including 45° (red) and 39° (black). Unpolarized sunlight would reflect with a 50% scaled version of the two polarization curves combined. Higher broadband reflectance is achieved at a larger incidence angle (blue).

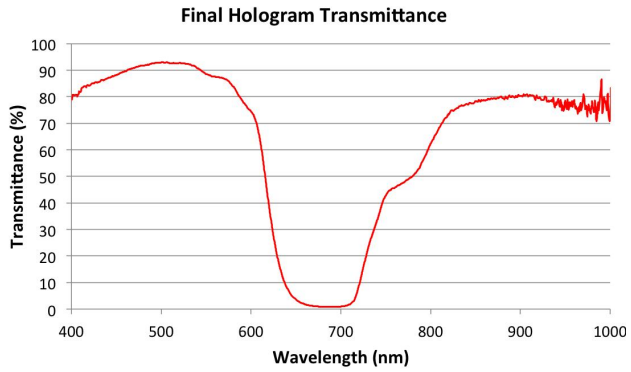

Figure 3. Spectral transmittance graph under unpolarized light for hologram design at desired wavelengh range. This curve is measured at 53° angle of incidence.

3. THEORETICAL ANALYSIS OF SPECTRUM SPLITTING SYSTEM

3.1 Spectral Conversion Efficiency

The exact location at which the hologram starts reflecting should correspond to the wavelength at which one PV cell produces a higher output power than the other PV cell. To determine this location, the spectral responsivity curves must be scaled by individual cell V_{OC} and FF values:

$$SCE(\lambda) = SR(\lambda) \cdot V_{OC} \cdot FF. \quad (1)$$

The resulting curve, called Spectral Conversion Efficiency (SCE), is shown in Figure 4. In this case, the SCE curves cross at 610 nm and the final hologram is designed to reflect between 610-800 nm.

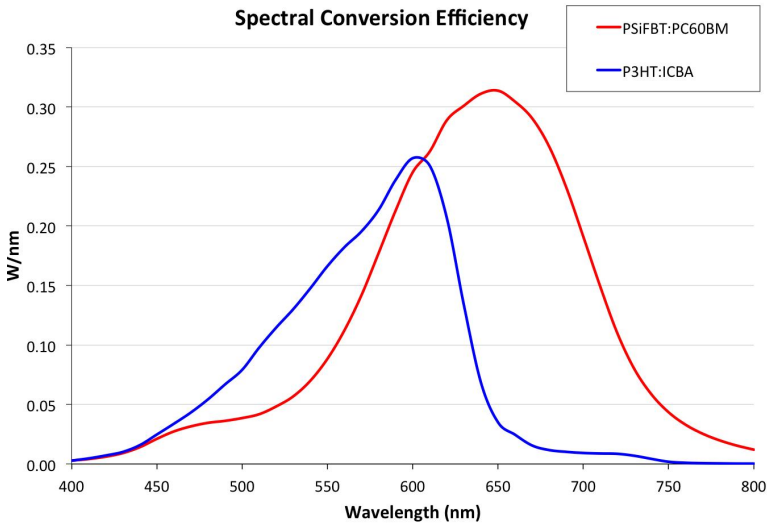

Figure 4. Spectral conversion efficiency of OPV cells in spectrum splitting system.

3.2 Improvement over Best Bandgap in Ideal Case

Before measuring the system, it is important to determine the best possible spectrum splitting performance for the OPV cells used. A spectrum splitting system shows improvement when its conversion efficiency or power output exceeds that

of the best performing cell under the full spectrum. Improvement over Best Bandgap (IoBB) is a figure of merit used to quantify percent improvement:

$$IoBB = \frac{\eta_{SS}}{\eta_{Best}} - 1 \quad (2)$$

$$IoBB = \frac{P_{SS}}{P_{Best}} - 1 \quad (3)$$

In this case the best cell is PSiFBT:$PC_{60}BM$, with η_{Best}=2.61% and P_{Best}=0.2867 mW.

The ideal spectrum splitting element would have 100% reflectance above 610 nm and 100% transmittance below 610 nm. To obtain theoretical best conversion efficiency, η_{Ideal}, the SCE for each PV cell is multiplied by this ideal filter and integrated over the spectrum. Theoretical IoBB under the reflection hologram is also calculated. In this case, the SCE curve of each PV cell is multiplied by T(λ) or R(λ)=(1- T(λ)-S) using the measured transmittance curve in Figure 3. A uniform scattering loss (S) of 3% in the film is assumed, and not counted toward the reflectance curve.

The system is measured under a Xenon arc solar simulator lamp. The spectral irradiance of the lamp varies from that of the sun, with a greater fraction of light in shorter wavelengths. It should be noted that this OPV-cell combination will operate at lower efficiency under a solar simulator compared to the sun due to relatively higher SCE values at longer wavelengths. Power output, theoretical conversion efficiency, and IoBB of the ideal spectrum splitting system and the holographic system are listed in Table 2. Results under the Xenon arc lamp and under sunlight are calculated separately to highlight differences.

Table 2. Power output, conversion efficiency and Improvement over Best Bandgap calculations for ideal and holographic spectrum splitting systems under a Xenon arc lamp and the sun.

AM 1.5D (Theoretical)				Xenon Arc Lamp (Theoretical)			
System	**P_{SS} (mW)**	**η_{SS}**	**IoBB**	**System**	**P_{SS} (mW)**	**η_{SS}**	**IoBB**
Ideal	0.3414	3.47%	26.38%	Ideal	0.3305	3.36%	22.34%
Holographic	0.3190	3.25%	18.08%	Holographic	0.3076	3.13%	13.87%

4. SYSTEM ASSEMBLY AND MEASUREMENT

The holographic beam-splitting setup was assembled and placed under a Xenon arc solar simulator lamp. The hologram was index-matched between two 45° glass prisms and rotated approximately 12° from the 45° orientation to achieve +/- 53° incidence in the glass medium (Figure 5). This angle of incidence corresponds to the transmittance spectrum shown in Figure 3. Current-voltage (I-V) curves of the OPV cells were measured under the full spectrum and in the spectrum splitting system. Ten I-V curves were taken and averaged for each measurement to eliminate the effect of lamp fluctuations. To represent a standard solar irradiance condition, the cells were positioned and the light level was adjusted until the I-V curve matched the electrical parameters in Table 1. Once the cells were positioned, the holographic beam splitter was added and I-V curves were taken under the filtered spectrum. Care was taken to ensure that incident light was uniform and that the exact same region of the hologram was used for reflective and transmissive I-V curve measurements.

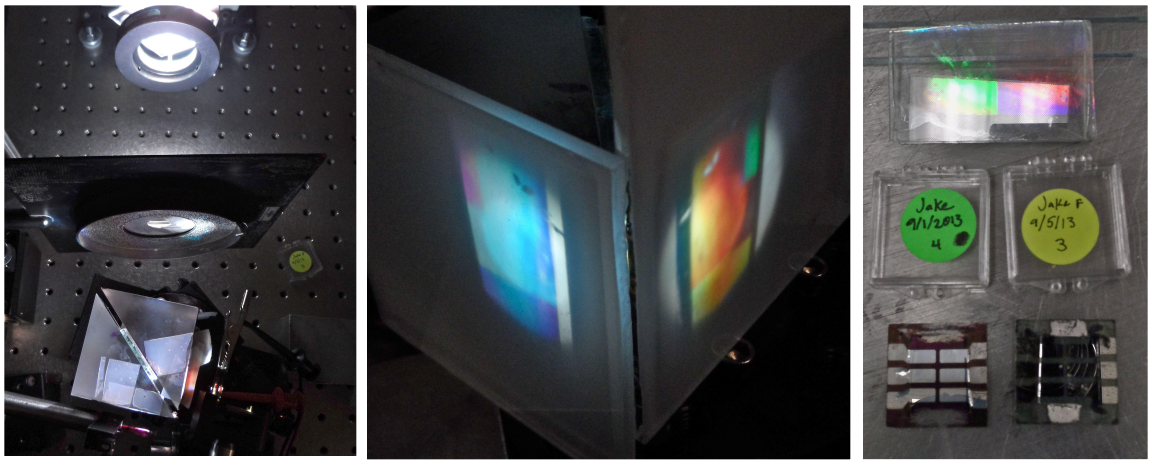

Figure 5. Measurement setup. Left: View from above of the solar simulator lamp and holographic spectrum splitting system. The hologram is placed between two 45° prisms with refractive index matching fluid. Center: Diffuse glass is placed at each output face of the prism to help visualize spectral distribution on each PV cell. Right: The reflection hologram and OPV cells used.

With I-V curves from each OPV cell under a full and filtered spectrum, measured system IoBB can be calculated,

$$IoBB = \frac{P_{SS1} + P_{SS2}}{P_{Best}} - 1 \tag{4}$$

where P_{SS1} and P_{SS2} are maximum power point measurements of each cell in the spectrum splitting system and P_{Best} is the maximum power point of the best performing solar cell under the full spectrum. A comprehensive list of results is shown in in Table 3.

Table 3. Theoretical and measured maximum power, conversion efficiency, and Improvement over Best Bandgap for spectrum splitting OPV system.

AM 1.5D (Theoretical)				Xenon Arc Lamp (Theoretical)				Xenon Arc Lamp (Measured)			
System	P_{SS} (mW)	η_{SS}	IoBB	System	P_{SS} (mW)	η_{SS}	IoBB	System	P_{SS} (mW)	η_{SS}	IoBB
Ideal	0.3414	3.47%	26.38%	Ideal	0.3305	3.36%	22.34%	Holo.	0.3034	3.09%	12.30%
Holo.	0.3190	3.25%	18.08%	Holo.	0.3076	3.13%	13.87%				

5. RESULTS

The assembled OPV spectrum splitting system outperforms either of its single cells under the full spectrum by 12.30%. This IoBB is just 1.57% below its predicted theoretical value under the solar simulator. Differences in predicted performance are likely due to measurement error and a slight underestimate of scattering loss. If scattering loss were increased to match the measured result (4.54% scattering), we can predict IoBB of 16.39% and conversion efficiency of 3.20% for the holographic spectrum splitting system under a true solar spectrum.

6. CONCLUSIONS

A successful OPV spectrum splitting system has been demonstrated using a reflective hologram as a spectral beam splitter. The combined system has a measured power and efficiency improvement over its best single OPV cell of 12.30% under a solar simulator lamp, with predicted improvement of 16.39% under sunlight. The performance would

increase further if the hologram had rectangular reflectance curve with no scattering. Under an ideal filter, this two-cell combination can achieve improvement of 26.38% in sunlight. If the solar cells chosen had equal conversion efficiencies and no overlap in spectral responsivity, the system could achieve up to 200% (2x) improvement in power output and efficiency. This holographic spectrum splitting concept can be applied to any two-cell combination including organic, inorganic, thin film, or a mixture of multiple types of PV.

REFERENCES

[1] Shockley, W., and Queisser, H. J., "Detailed balance limit of efficiency of p-n junction solar cells," Journal of applied physics 32(3), 510-519 (1961).

[2] Green, M. A., et al. "Solar cell efficiency tables (version 39)," Progress in photovoltaics: research and applications 20(1), 12-20 (2012).

[3] Hadipour, A., de Boer, B., and Blom, P. W. M. "Organic tandem and multi-junction solar cells," Advanced functional materials 18(2), 169-181 (2008).

[4] You, Jingbi, et al. "A polymer tandem solar cell with 10.6% power conversion efficiency," Nature communications 4, 1446 (2013).

[5] Zhang, D., et al. "Reflection hologram solar spectrum-splitting filters," Proc. SPIE 8468, 846807 (2012).

[6] Yuan, M., Yang, P., Durban, M. M., and Luscombe, C. K., "Low bandgap polymers based on silafluorene containing multifused heptacylic arenes for photovoltaic applications," Macromolecules 45(15), 5934-5940 (2012).

[7] Chang, Byung Jin, and Carl D. Leonard. "Dichromated gelatin for the fabrication of holographic optical elements," Applied optics 18(14), 2407-2417 (1979).